Science Bulletin 66 (2021) 2238–2250

Contents lists available at ScienceDirect

Science Bulletin

journal homepage: www.elsevier.com/locate/scib

Science Bulletin
www.scibull.com

Article

Characterization of exploratory patterns and hippocampal–prefrontal network oscillations during the emergence of free exploration

Wenxiu Dong [a], Hongbiao Chen [a], Timothy Sit [a], Yechao Han [a], Fei Song [b,c,d], Alexei L. Vyssotski [e], Cornelius T. Gross [f], Bailu Si [g,*], Yang Zhan [a,*]

[a] Guangdong Provincial Key Laboratory of Brain Connectome and Behavior, CAS Key Laboratory of Brain Connectome and Manipulation, the Brain Cognition and Brain Disease Institute (BCBDI), Shenzhen Key Laboratory of Translational Research for Brain Diseases, Shenzhen Institutes of Advanced Technology, Chinese Academy of Sciences, Shenzhen-Hong Kong Institute of Brain Science-Shenzhen Fundamental Research Institutions, Shenzhen 518055, China
[b] State Key Laboratory of Robotics, Shenyang Institute of Automation, Chinese Academy of Sciences, Shenyang 110016, China
[c] Institutes for Robotics and Intelligent Manufacturing, Chinese Academy of Sciences, Shenyang 110169, China
[d] University of Chinese Academy of Sciences, Beijing 100049, China
[e] Institute of Neuroinformatics, the University of Zürich and Swiss Federal Institute of Technology (ETH), Zurich CH-8057, Switzerland
[f] European Molecular Biology Laboratory (EMBL), Monterotondo 00015, Italy
[g] School of Systems Science, Beijing Normal University, Beijing 100875, China

ARTICLE INFO

Article history:
Received 30 October 2020
Received in revised form 20 March 2021
Accepted 18 May 2021
Available online 24 May 2021

Keywords:
Exploration
Prefrontal cortex
Hippocampus
Neural oscillations
Entropy

ABSTRACT

During free exploration, the emergence of patterned and sequential behavioral responses to an unknown environment reflects exploration traits and adaptation. However, the behavioral dynamics and neural substrates underlying the exploratory behavior remain poorly understood. We developed computational tools to quantify the exploratory behavior and performed *in vivo* electrophysiological recordings in a large arena in which mice made sequential excursions into unknown territory. Occupancy entropy was calculated to characterize the cumulative and moment-to-moment behavioral dynamics in explored and unexplored territories. Local field potential analysis revealed that the theta activity in the dorsal hippocampus (dHPC) was highly correlated with the occupancy entropy. Individual dHPC and prefrontal cortex (PFC) oscillatory activities could classify various aspects of free exploration. Initiation of exploration was accompanied by a coordinated decrease and increase in theta activity in PFC and dHPC, respectively. Our results indicate that dHPC and PFC work synergistically in shaping free exploration by modulating exploratory traits during emergence and visits to an unknown environment.

© 2021 Science China Press. Published by Elsevier B.V. and Science China Press. All rights reserved.

1. Introduction

Exploration is a common behavior when individuals enter a new environment. It underlies many cognitive functions, such as active sensing, perception, and spatial cognition. The emergence of exploration is driven by curiosity and motivational purposes, such as novelty seeking, learning, and uncertainty resolving [1–3]. Unlike exploration in maze studies using limited exploratory space in which animals are subject to food or water constraints, exploration under free conditions comprises the emergence of naturalistic exploratory behavior in a novel environment and therefore permits the investigation of the neural substrates underlying natural voluntary behavior. Previous investigations on free exploration have shown that rodents display an intentional drive to explore large unknown environments with dynamic and sequential exploratory patterns [4]. Individuals exploring novel environments can be active or passive explorers highlighting individualized coping strategies or behavioral traits [5]. Previous studies have shown that forced exploration in small environments differs significantly from free exploration in large environments. However, few analytical tools are available to quantify this complex behavior, and the brain mechanisms underlying such behavior are less understood.

The hippocampus (HPC) regulates navigation in a given environment. Lesion of HPC impairs the exploratory behavior of rats [6]. In addition, prefrontal cortex (PFC) neural activity is synchronized with the HPC in exploring different dimensions of the environment, including anxiety-related measures of center vs. wall in the open field [7] or close vs. open portions of a maze [8,9] or location-related measures of task-learning rules [10,11]. These studies have demonstrated the importance of coordinated oscillations in the HPC and PFC; through synchronization or coactivation,

* Corresponding authors.
E-mail addresses: bailusi@bnu.edu.cn (B. Si), yang.zhan@siat.ac.cn (Y. Zhan).

https://doi.org/10.1016/j.scib.2021.05.018
2095-9273/© 2021 Science China Press. Published by Elsevier B.V. and Science China Press. All rights reserved.

the two areas participate in processing different aspects during exploration and possibly incorporate cues from other brain regions.

Exploration is a dynamic process intermingled with habituation [12]. The spatial–temporal pattern of exploration results from various factors, such as novelty seeking or risk avoidance [5,13]. Most descriptions of exploration focused on the thigmotaxic division of the test field, and exploratory patterns in a large unknown environment have few quantitative or statistical measures. In addition, few studies related exploration to neural activities. How oscillatory and synchronized activities in the hippocampal–prefrontal circuit process different aspects of self-initiated free exploration is intriguing to investigate. The hippocampal and prefrontal systems possibly use oscillatory activities to drive exploration and perform dynamic representations of the environment and further guide the exploratory behavior.

In this work, we characterized free exploration by defining occupancy entropy from the probabilistic distribution of animals' location time series. Furthermore, wireless local field potential (LFP) recordings were made simultaneously in the ventral HPC (vHPC), dorsal HPC (dHPC), and PFC when the animals performed free exploration. We aim to provide insights into the dynamic patterns of exploration by developing quantitative tools and understand how hippocampal and prefrontal oscillatory activities modulate exploration.

2. Materials and methods

2.1. Animals

C57BL/6J mice were purchased from Charles River Laboratories (Calco, Italy). Animals were housed in ventilated cages and stored on a 12 h/12 h light–dark cycle (lights on at 7 a.m.) with temperature (21.5 °C ± 1 °C) and humidity (55% ± 8%). Food and water were available ad libitum. This study was approved by the animal ethics committee of European Molecular Biology Laboratory (EMBL) and the Italian Ministry of Health (541/2015-PR), and experiments were carried out in accordance with the National Institute of Health guide for the care and use of laboratory animals.

2.2. Electrophysiology

Mice (3–6 months old) were used for electrophysiological recordings. The animals were anesthetized with a mixture of ketamine and xylazine (100 and 10 mg/kg) and placed on a heating pad to maintain the body temperature at 35 °C. The head was fixated on a stereotaxic with a microscope. Supplemental inhaling isofluorane was provided. An incision was cut above the skull, and burr holes were drilled at the dHPC (bregma as reference and depth was relative to the brain surface, 1.9 mm posterior, 1.4 mm lateral, and 1.35 mm depth), the vHPC (3.1 mm posterior, 3.2 mm lateral, and 3.9 mm depth), and the PFC (1.8 mm anterior, 0.5 mm lateral, and 1.5 mm depth). Tungsten wire electrodes (Advent Research Materials, Oxford, UK) were advanced into the brain at the above locations. Two additional miniature screws were anchored on the posterior and anterior portions of the skull as ground and reference, respectively. The electrode wires were inserted into a 7-pin connector, which served as an interface for neurologger recording. Dental cement was carefully applied over the skull to form a head stage that protects the electrodes and wires. After surgery, the animals were housed individually and allowed at least 1 week to recover. Before the recordings, the animals were habituated to the installing of the neurologger for 3 d using a dummy neurologger with a similar weight and shape. LFP signals were collected using a wireless neurologger system [14]. The sampling frequency for the LFP signals was 1600 Hz. After the recordings, electrolytic lesions were made and the brains were dissected.

2.3. Emergence test and behavioral tracking

To study the exploration behavior under naturalistic conditions similar to those encountered by animals in nature, we established a large arena connected to a home shelter, allowing animals to explore freely by their own intentions. Details of the experimental apparatus are described in Ref. [15]. The arena consisted of a circular open field with a wall covered by an opaque curtain. The arena was approximately 1.8 m in diameter and 12 cm in wall height. An overhead camera was mounted on the ceiling to monitor the exploratory behavior. The arena was connected to a home cage through a small opening. The arena and the home were separated by a removable shutter. The home cage contains a portion of the bedding from the home cage where the animal usually lived. This home cage served as a habitat when the animal made excursions into the arena and returned from it. The experiment started by transferring a mouse into the experiment room. The neurologger recording chip was inserted into the pins on the head stage of the animal. Then, diazepam (DZP, 1 mg/kg) or vehicle (VEH) was treated through intraperitoneal injection. The mouse was then placed into the home cage of the emergence test. The mouse stayed in the home for 15 min, and the removable shutter was opened afterward. The experiment continued for 80 min. The behavior was tracked using Viwer2 software (Biobserve, St. Augustin, Germany). The video frame rate was 25 Hz. The video tracking and the neurologger recording were synchronized through the built-in infrared receiver on the neurologger. The behavioral tracking data were analyzed using the SEE package. SEE software separates the tracking data into the wall and the center [16,17].

The animals visited the arena and returned to the home cage frequently, and each round trip was referred to as an excursion. Considering that the animals spent a large portion of time around the home opening, we fitted the total 80 min positional data with a two-dimensional Gaussian distribution and defined the area covering 95% of the probability density mass from the home cage as the garden area. The group of explorer mice, which emerged from the home cage and explored the arena, comprised four animals from the DZP group and four animals from the VEH group. The group of home-only mice, which stayed in the home only and did not enter the arena, comprised four animals from the DZP group and eight animals from the VEH group.

2.4. Spectral and time–frequency analysis

The LFPs were analyzed by multi-taper analysis using the Chronux package [18]. Data were downsampled to 400 Hz, and the 50 Hz line was removed using a notch filter. The whole duration of LFP data was subjected to time–frequency analysis to extract different frequency bands. The moving window length was 2 s, with step 0.04 s. The tapers and time–frequency bandwidth were set as params.tapers = (3, 5). Zeros were padded at the two ends of the data with the length of half size of the moving window. This step produced a time–frequency transformed power or coherence with the same temporal length as the behavioral tracking data (80 min data at 25 Hz having 120,000 data points). The frequency band was divided into delta (1–4 Hz), theta (4–12 Hz), beta (15–25 Hz), and gamma (30–80 Hz) bands, and the average was taken within each band.

The LFP was extracted at four speed ranges: 0–5, 5–10, 10–15, and 15–20 cm/s. The analysis was confined to the excursion trips while the animals performed exploration in the arena. Speeds less than 20 cm/s covered 84.7% ± 5.9% (mean ± standard deviation (SD)) of all traveling speeds in all mice. The average speed was

6.3 ± 2.8 (mean ± SD) cm/s. Immobility at speed equal to 0 was excluded in the LFP analysis. For the analysis of LFP power across time windows, the power was averaged across excursions, and all excursions were combined across the animals. On average, for each animal, 2–8 excursions were included in the VEH group and 9–17 excursions were included in the DZP-treated group during a given 10 min time window.

2.5. Occupancy entropy

We defined and calculated occupancy entropy from the animal's positional time series in a large environment to quantify the exploratory dynamics. The arena was divided into 100 by 100 spatial bins covering the circular arena. Each bin represents a state of location. For a given spatial bin, we calculated the visits to this bin as cumulative occupancy across time. If the animal stayed in a bin for consecutive times, the number of visits increased with time. The number of visits to the i-th bin up to time t was calculated as

$$C_c(i,t) = \sum_{\tau=0}^{t} \delta_{x_\tau \in b_i}, \tag{1}$$

where δ is an indicator function, whose value is 1 if the condition is true. x_τ is the position of the animal at time τ. b_i is the area of the i-th spatial bin. During time 0 – t, the access probability of the i-th bin over the spatial bins is

$$O_c(i,t) = \frac{C_c(i,t)}{\Sigma_j C_c(j,t)}. \tag{2}$$

The cumulative occupancy entropy was defined by the probability over the spatial bins and calculated as

$$E_c(t) = -\sum_i O_c(i,t)\log_2 O_c(i,t). \tag{3}$$

To measure the exploration behavior in a short time period, we counted the number of visits to spatial bins in a time window of length l

$$C_l(i,t) = \sum_{\tau=-l/2}^{l/2} \delta_{x_{t+\tau} \in b_i}. \tag{4}$$

The local occupancy probability was given by

$$O_l(i,t) = \frac{C_l(i,t)}{\sum_j C_l(j,t)}, \tag{5}$$

and the corresponding local occupancy entropy was

$$E_l(t) = -\sum_i O_l(i,t)\log_2 O_l(i,t). \tag{6}$$

Following the convention, $0\log_2 0$ is defined as 0 when calculating entropy. The occupancy entropy reaches the minimal value 0 when the occupancy is a Dirac delta distribution, i.e., the probability density concentrates in one spatial bin. The maximal occupancy entropy is achieved by the uniform occupancy over the spatial bins, and the value is $\log_2(100 \times 100) = 13.29$. For the calculation of local entropy, the moving window length was 30 s. The cross-correlation values between the local entropy and the theta power were taken as the average in the range of −5 to 5 s.

2.6. Analysis of explored and unexplored areas

During exploration, the prior unknown arena is gradually becoming familiar. We quantified the area that had already been explored and that was previously unexplored, i.e., the newly explored area, in the current excursion. We divided the area into 40 × 40 bins, and the bin size was 5 cm × 5 cm. This bin size should cover the size of the body area and be comparable to the size of the mouse. The explored areas of the excursion were defined as those bins that were visited in previous excursions. The unexplored areas of the excursion were defined as the bins that were never visited in previous excursions. Then, we labeled the behavior time series corresponding to the exploratory path as explored or unexplored according to whether it fell into the explored or unexplored bins.

2.7. Classification using a decision tree

We used vHPC, dHPC, and PFC power and coherence from four frequency bands as features to classify the exploratory categories of wall vs. center, explored vs. unexplored, and in vs. out of the garden. Decision tree models were built to classify the three behavioral paradigms [19]. The use of decision tree models was motivated by their ability to capture nonlinear relationships and their Whitebox model approach [19]. The feature matrix consisted of 24 power and coherence features from 4 frequency bands of theta, delta, beta, and gamma from the 3 brain areas. For each classification task, a binary label was created based on mouse behavior, and equal amounts of data for two classes were selected. To evaluate the classification performance of each decision tree, we used a randomly selected training set consisting of 60% of our total feature matrix and a testing set consisting of 40% previously unselected labels. Final classification accuracy was determined by averaging the performance of decision trees based on this hold-out validation method for 100 iterations. Decision trees were trained using MATLAB's fitctree function. The maximum number of splits of tree models was set to 5000 to limit the complexity of our models, and split predictors were selected via the interaction test method to increase the detection of interactions between important predictors. The predictor importance of features was estimated using the predictor importance function of MATLAB. The function computes the summation of the changes in the mean squared error because of splits on every predictor and divides this by the total number of branch nodes. The changes in mean squared error are estimated by multiplying the Gini impurity by the node probability. Our tree models were grown without surrogate splits; hence, this sum was taken over the optimum splits found at each branch node. Gini impurity measures the probability that a randomly chosen element in our label vector will be misclassified if it is classified based on the distribution of the categories in our label vector. It is computed by multiplying the probability of choosing that element by the probability of misclassification [20].

2.8. Statistics

The overall mean was taken over the number of excursions from all mice to analyze the drug effects on entropy or power. Analysis of variance (ANOVA) was used, followed by a post-hoc test. Paired t-test was used to analyze power or coherence changes before and after garden transitions. For the theta power comparison between explorer mice and the home-only mice, the mean was taken over the number of mice. Repeated-measures ANOVA was used to evaluate the power changes after shutter opening.

3. Results

3.1. Characterization of exploratory activity in free exploration

A naturalistic setup (Fig. S1a online) consisting of a home base and a large exploration field was established to allow the animals to perform free exploration of an external environment similar to their ecological settings [4]. This setup was used to investigate

the spontaneous exploratory behavior of individual mice and measure the exploration in the open arena for a long period (Fig. S1b online). Mice started in the home and a movable shutter between the arena wall and the home was removed after a period of habituation (Fig. S1b online). Naturally, the mice left the small opening on the arena wall and displayed a willingness to explore the arena [21]. The exploration behavior started with leaving the home and traveling along the arena wall near the home and then followed by the gradual buildup of exploration with more occupation of the arena (Fig. 1a). This phenomenon is reflected by the patterned exploration path and angular spread in four successive 20 min intervals out of the total 80 min exploration (Fig. 1b).

As shown in Fig. 1a, the mice preferred to explore along the wall near the home, and they visited more locations as time was prolonged. To quantify the overall exploratory pattern over time, we defined cumulative occupancy entropy by determining the entropy of the occupancy distribution (see methods). Cumulative occupancy entropy measures how the visiting locations are distributed as exploration time progressed. Low cumulative occupancy entropy indicates the concentrated visits to some locations, whereas the maximal occupancy entropy corresponds to the same number of visits to all locations. After over 80 min, the cumulative occupancy entropy showed a gradient increase (Fig. 1c), demonstrating that the mice gradually explored the arena with small-scale concentrated visits evolving into regular distributed visits in the arena.

To quantify the exploratory patterns on a moment-by-moment basis, we defined local occupancy entropy by computing the occupancy distribution of exploration locations in a local time window centered at the current time (Fig. 1d). A high local occupancy entropy value indicates the exploration behavior that covers an area uniformly, while zero local occupancy entropy indicates immobility or returning to the home base in a given short time. The local occupancy entropy showed fluctuations, capturing the time-dependent changes of exploratory extent. The peak values of local occupancy entropy had an increasing trend, indicating an increasing exploratory motivation. The local occupancy entropy value dropped to zero from time to time, characterizing the moments when the animal returned to the home base or remained immobile.

3.2. Characterization of altered exploration patterns with behavioral perturbations

To confirm whether or not our entropy measurements can capture different exploration patterns, we perturbed the exploratory behavior of the animals. We treated the animals with DZP, a previously validated drug that causes behavioral changes in the free exploration test [15]. We computed the average entropy of all excursions in the DZP-treated group and in the VEH-treated group. As the test time was prolonged, the cumulative entropy in both groups gradually increased over time (Fig. 1e). A significant treatment-by-time interaction was observed after over 80 min (drug by time: $F_{(7,\ 527)} = 16.67$, $P < 0.000001$), demonstrating that the cumulative entropy in the two groups had different patterns at different times. During 0–30 min, the cumulative entropy in the DZP group was higher than that in the VEH group; during 30–70 min, the cumulative entropy was not different between the two groups (Fig. 1e). The increase in the cumulative entropy during the initial stage indicates that the drug treatment enabled the animals to make early exploratory visits to the arena with strong motivation.

We next examined how the drug perturbation affected the local occupancy entropy. The local entropy also increased with time in both groups ($F_{(7,\ 527)} = 8.26$, $P < 0.00001$). Between the two groups, the local entropy was different ($F_{(7,\ 527)} = 60.16$, $P < 0.000001$), confirming that local entropy could capture the moment-to-moment exploration changes by the drug perturbation. A significant treatment-by-time interaction was also observed for the local entropy ($F_{(7,\ 527)} = 3.17$, $P = 0.003$). The local entropy in the DZP group decreased after 20–30 and 40–70 min (Fig. 1f), indicating that local exploration was less random. Compared with the VEH group, the DZP group made more frequent visits to the arena with reduced time spent in the home between two successive excursions in the arena (Fig. 1g). The decrease in local entropy at a later time during the exploration indicated that local exploration occurred in a regular route instead of a distributed route under the drug treatment.

3.3. Exploration in the explored areas vs. unexplored areas

Navigation in unexplored areas forms the basis to establish spatial memory [22,23] and reflects learning and coping strategies in finding rewards and expecting dangerous threats [24]. A small open field setup cannot disclose the exploration patterns in unknown areas because animals in a small space occupy the entire arena quickly. We therefore aim to understand the exploratory dynamics in the areas not previously visited by the animals. We defined the unexplored areas as those the animals had just visited for the first time during the current excursion and the explored areas as those the animals had already visited in previous excursions (Fig. 2a). As the mice made more excursions in the arena, the proportion of the traveling path in the unexplored areas decreased and the proportion in the explored areas increased (Fig. 2b). This result demonstrates that the mice became more familiar with the environment in a buildup fashion. The overall proportion of the explored and unexplored areas after over 80 min was different between the DZP and VEH groups (Fig. 2c), demonstrating that drug perturbation can influence the exploration in the two areas.

Next, we examined the entropy measurements in the explored and unexplored areas. In the explored areas, the local entropy showed different patterns over time between the VEH and DZP groups (Fig. 2d). During the first 20 min, the local entropy in the explored areas was not different between the two groups. During the 20–80 min period, the local entropy decreased in the DZP group compared with the VEH group. In the unexplored areas, the local entropy did not significantly differ between the VEH and DZP groups, indicating that the exploration patterns were unaffected by the drug perturbation. These data demonstrate that exploration in explored and unexplored territories can reveal the differential patterns of perturbed exploratory dynamics.

3.4. Modulation of exploration by dHPC theta power

To understand the neural activity changes during free exploration, we implanted microwire electrodes in the dHPC, the vHPC, and the PFC for LFP recordings (Fig. S2a, b online) by using a wireless neurologger system [25]. The wireless neurologger was well suited for our large-arena settings in which the mice frequently transited through the small opening in the wall between the arena and the home. The LFPs were subjected to multi-taper time–frequency analysis to examine theta band (4–12 Hz) oscillatory activities (Fig. S2c and Fig. S3a online). The dHPC theta power gradually increased with time during the emergence test period (Fig. 3a). The pattern was consistent for different speed ranges. The theta power in the vHPC and the PFC did increase with time (Fig. S3b, c online). To understand the relationship between the exploration pattern and the theta activity, we computed the cross-correlation from the time series between the local entropy and theta power from the three brain areas. The cross-correlation between the dHPC power and the local entropy (dHPC–LE) showed a prominent peak,

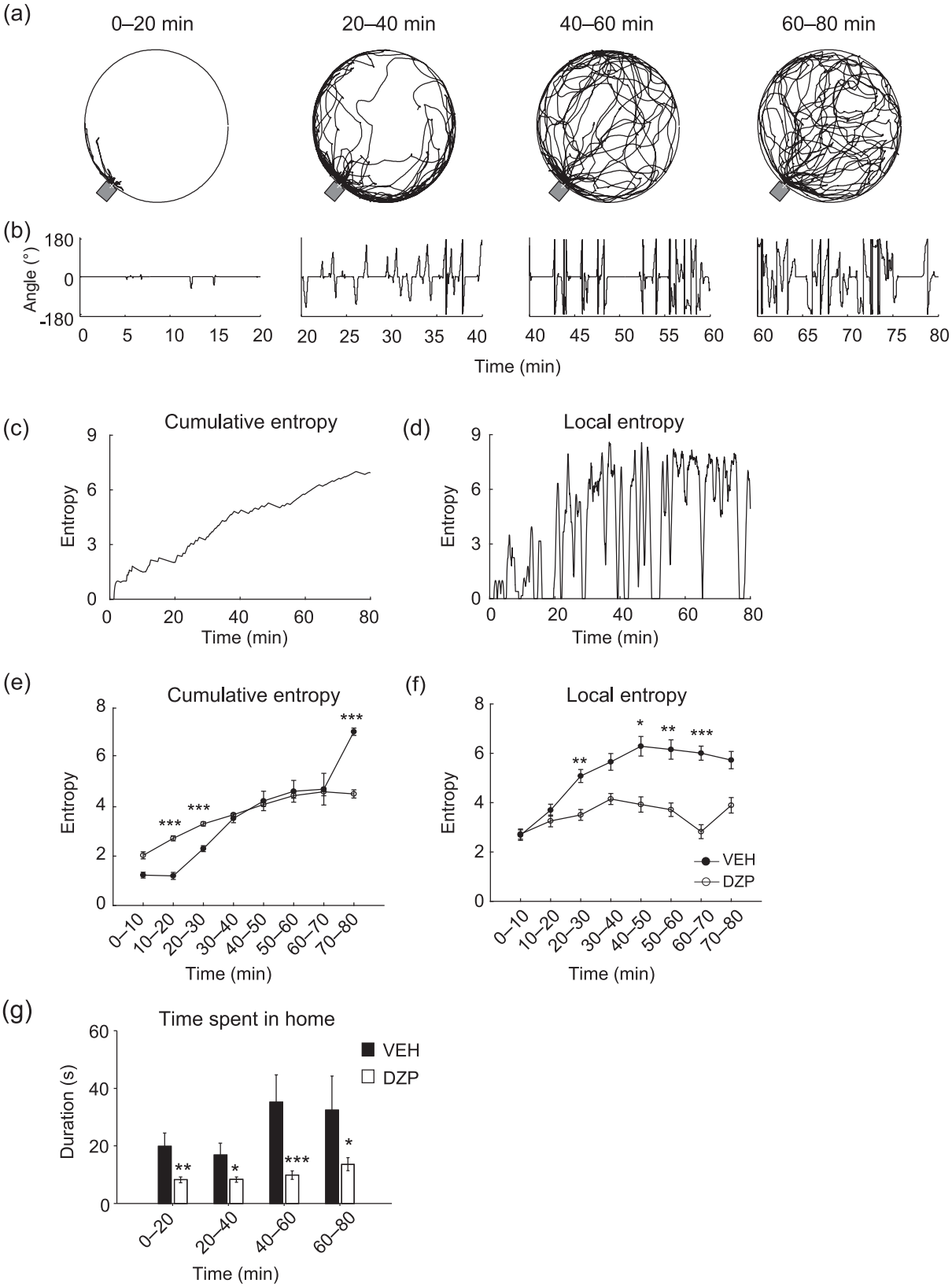

Fig. 1. Characterization of exploration behavior in a naturalistic arena setup. (a) Representative exploration behavior in the arena. In the first 20 min, the mice started leaving the home shelter and explored near the opening area. In the subsequent 20-min intervals, the exploration gradually expanded into the full circle around the wall and the center of the arena. (b) The angular position of the mouse represented by the angles away from the home shelter, using the arena center as the central point. Positive angles represent clockwise exploration, and negative angles represent counter-clockwise exploration. (c) Example of cumulative occupancy entropy (CE) describing the exploration behavior during an 80-min test. (d) Example of local occupancy entropy (LE) of exploration showing the local coverage in the arena. (e) Perturbation of the exploration by diazepam quantified by CE in 20 min time bins. ANOVA, Drug: $F_{(7,\ 527)} = 102$, $P < 0.000001$. (f) Perturbation of the exploration by diazepam quantified by LE. ANOVA: $F_{(7,\ 527)} = 8.26$, $P < 0.00001$. (g) Duration of time spent in the home between successive excursions in the arena under the treatment of vehicle or diazepam. ANOVA, Drug: $F_{(1,\ 802)} = 55.58$, $P < 0.0001$. * $P < 0.05$, ** $P < 0.01$, *** $P < 0.001$, VEH vs. DZP, Bonferroni correction. The data are shown as mean ± standard error of the mean (SEM).

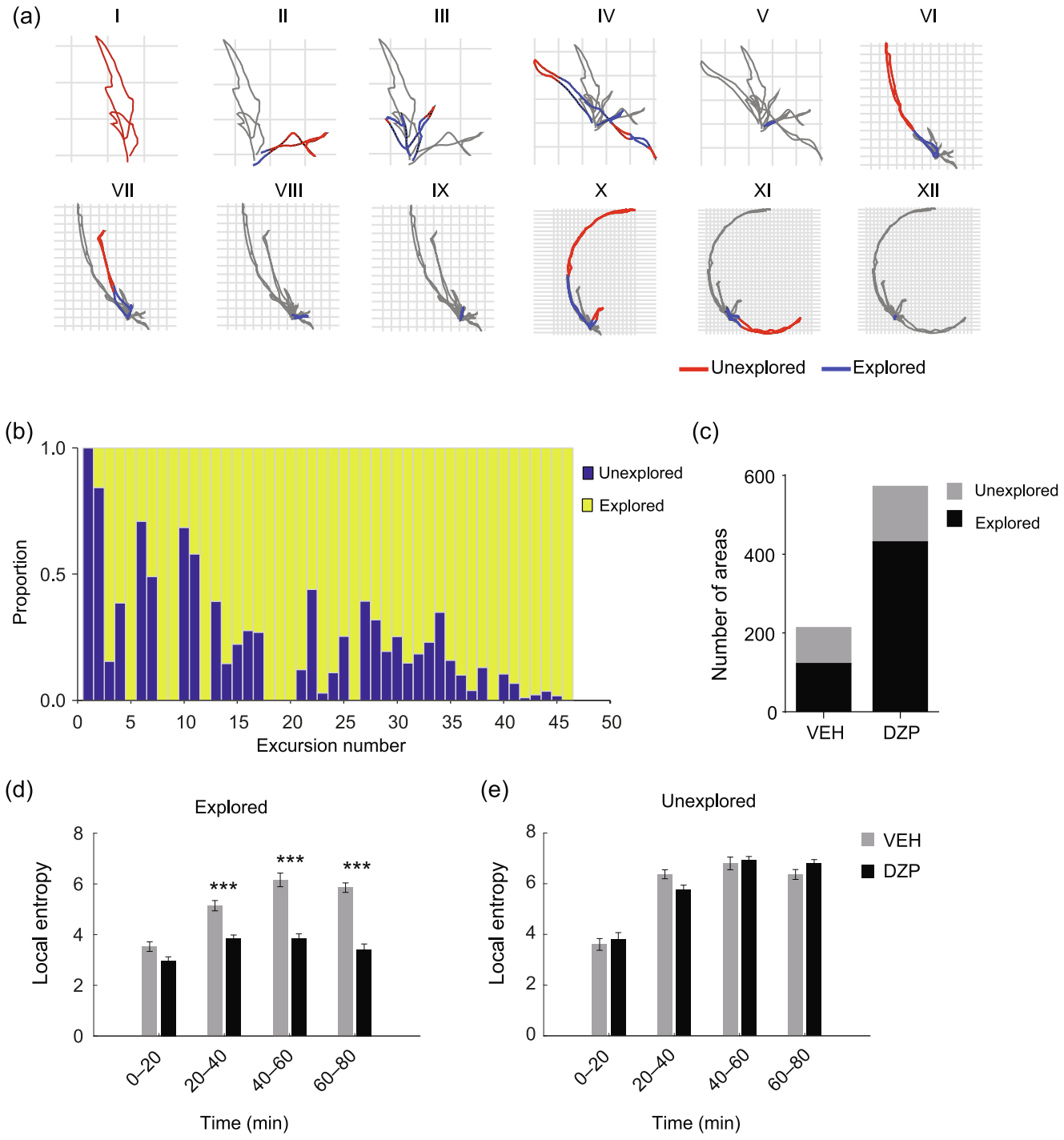

Fig. 2. Characterization of explored and unexplored areas and selective effects of diazepam on explored areas. (a) Definition of explored and unexplored areas during each excursion in the arena. Successive excursions were shown from panel I to XII. (b) Example showing the development of explored/ unexplored proportion for the total excursions. (c) Distribution of explored and unexplored areas in the two groups, $\chi^2(10) = 25.56$, $P = 0.004$. (d) Development of the LE in the explored areas in 20 min bins. Significant effect of diazepam was found. ANOVA, time: $F_{(1, 537)} = 7.49$, $P < 0.0001$, drug: $F_{(1, 537)} = 1.71$, $P = 0.19$, time by drug: $F_{(1, 537)} = 4.9$, $P < 0.001$. (e) Development of the local entropy in unexplored areas in 20 min bins. No effect of diazepam was found. ANOVA, time: $F_{(1, 224)} = 28.65$, $P < 0.0001$, drug: $F_{(1, 224)} = 42.13$, $P < 0.0001$, time by drug: $F_{(1, 224)} = 1.04$, $P = 0.38$. *** $P < 0.001$, VEH vs. DZP, Bonferroni correction. The data are shown as mean ± standard error of the mean (SEM).

in contrast to vHPC–LE and PFC–LE correlations (Fig. 3b). The length of the local window used for the calculation of the local entropy did not affect the magnitude of correlation (Fig. S4a online; $F_{(5, 90)} = 0.6993$, $P = 0.63$). We observed a reliable and tight temporal relationship as the peak time for the dHPC–LE cross-correlation could closely follow the local window shift (Fig. S4b online). dHPC had a stronger correlation with the local exploration than the other brain areas of vHPC and PFC (Fig. 3c). Strong correlations were also present in the DZP group (Fig. 3d). We also calculated the dHPC–LE correlation in different speed ranges from 0 to 20 cm/s in the 5 cm/s bin. We did not observe a speed effect on the dHPC–LE correlation (VEH: $P = 0.51$, $F_{(3, 36)} = 0.78$; DZP: $P = 0.52$, $F_{(3, 36)} = 0.77$), indicating that speed does not confound the correlation between the local entropy and the dHPC power

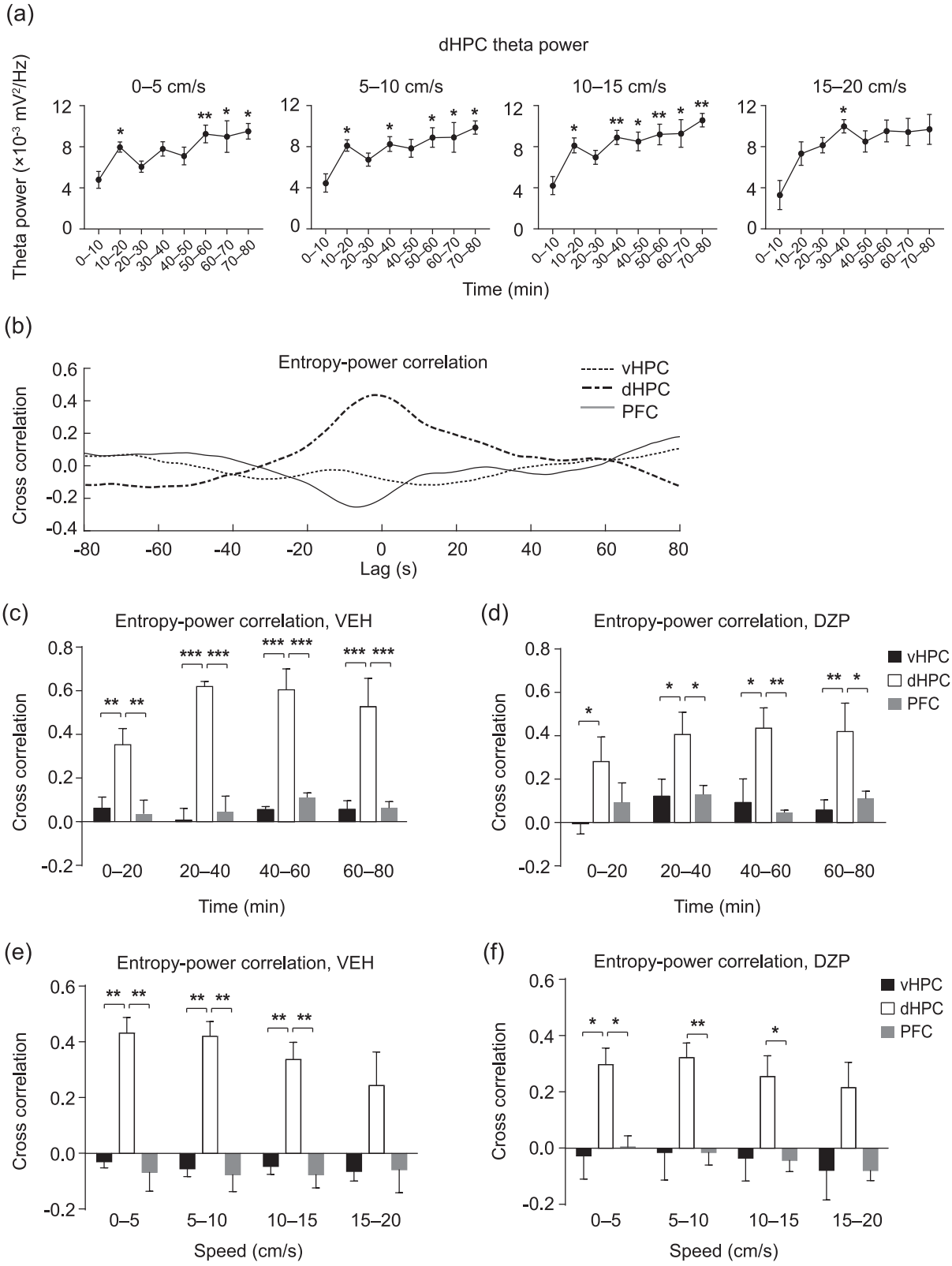

Fig. 3. Modulation of local occupancy entropy by dHPC theta power. (a) dHPC theta power changes with time in the emergence test for different speed ranges. The theta power was averaged across excursions combined from all the animals. Speed 0–5 cm/s, ANOVA, time: $F_{(7,\ 110)} = 3.485$, $P = 0.0021$, speed 5–10 cm/s, time: $F_{(7,\ 108)} = 2.562$, $P = 0.0176$, speed 10–15 cm/s, time: $F_{(7,\ 101)} = 3.063$, $P = 0.0058$, speed 15–20 cm/s, time: $F_{(7,\ 85)} = 1.940$, $P = 0.073$. Bonferroni correction time 0–10 mins vs. other time points. (b) Example of cross-correlation analysis between local entropy and theta power in the areas of vHPC, dHPC, and PFC. The time lag was in the range of −80 to 80 s. The local window size was 30 s. (c, d) Comparison of cross-correlation strength between the theta power in the three brain areas and the local entropy showing the highest cross-correlation between dHPC power and local entropy. Cross-correlation values were calculated as the average in the range of −5 to 5 s. (c) VEH group. ANOVA, brain area: $F_{(2,\ 36)} = 71.43$, $P < 0.0001$; (d) DZP group. ANOVA, brain area $F_{(2,\ 36)} = 18.09$, $P < 0.0001$. Bonferroni correction dHPC vs. other brain areas. (e, f) Cross-correlation between local entropy and theta power at different speed ranges. (e) VEH group. ANOVA, $P = 0.51$, $F_{(3,\ 36)} = 0.78$; (f) DZP group. ANOVA, $P = 0.52$, $F_{(3,\ 36)} = 0.77$. * $P < 0.05$, ** $P < 0.01$, *** $P < 0.001$, dHPC vs. other brain areas, Bonferroni correction. The data are shown as mean ± standard error of the mean (SEM).

(Fig. 3e, f). The strong correlation suggests that dHPC theta power is an indicator of local exploration behavior.

3.5. PFC–dHPC coherence signals garden exit and return

After the mice left the home, the mice spent a considerable amount of time in the area around the opening, and this area was referred to as a "garden" [21]. Previous studies have reported that leaving the garden may reflect a key decision state for the mice to explore the arena [15]. We then tested whether or not LFPs change during transitions between the garden area and the area out of the garden. To quantitatively characterize the garden area, we fitted the dwell time for 80 min by using a two-dimensional Gaussian distribution. The garden area was then defined as the 95% confidence levels from the cumulative distribution (Fig. S6a online). We extracted the behavioral epochs when the animals left the garden and the epochs when the animals returned to the garden from the outside area (Fig. 4a). LFP power and coherence were analyzed during the garden transitions. The coherence between the PFC and dHPC increased after the mice left the garden (Fig. 4b). Correspondingly, the PFC–dHPC coherence decreased after the mice returned to the garden (Fig. 4c). Coherence under the DZP treatment showed the same patterns during garden transitions (Fig. 4b, c), and the coherence values in the two groups were not different (Fig. 4d). In addition, PFC–dHPC coherence was not different at different speed ranges (Fig. S6e online). These data revealed that PFC–dHPC coherence signaled the transitions when the animals decided to leave and enter the garden area.

The theta power in the dHPC increased when the mice left the garden and decreased when the mice entered the garden (Fig. 4e). However, the changes in power during garden transitions could not be segregated from the changes in speed because outward and inbound travels were associated with acceleration and deceleration, respectively (Fig. S6d online). Power in the DZP group differed from that in the VEH group, reflecting that the drug affected the theta activity (Fig. S5 online). PFC or vHPC power did not show changes during in/out garden transitions (Fig. S6b, c online). The fact that the dHPC power shows a similar pattern to the PFC–dHPC coherence indicates that theta power changes might have confounding effects with coherence.

3.6. Prediction of multiple exploratory dimensions by dHPC and PFC power

The occupancy entropy correlated with the dHPC oscillatory activity and synchronization between the PFC and the dHPC signaled the transitional exploration in the garden area. Thus, we tested whether or not individual and correlated oscillatory neural activities between these brain areas can predict various aspects of exploration. We performed machine learning classification of oscillatory features in explored vs. unexplored areas (Fig. 5a), in vs. out of the garden areas (Fig. S6a online), and wall vs. center areas (Fig. S7a online). These categories were regarded to indicate different behavioral dimensions because the wall/center areas are frequently used to indicate levels of anxiety, the explored/unexplored areas we defined involved novel and unknown spatial processing, and in/out the garden areas involved decision making.

We performed the classification using a combination of power and coherence measurements from four frequency bands out of the dHPC, vHPC, and PFC. In total, 24 features were obtained, which were then used to train the classifier and to classify the three exploratory categories. These predictors could classify three categories reliably with high accuracy (Fig. 5a and Fig. S7b online). When the features of power and coherence were separately used for the classification, we found that power outperformed coherence (Fig. 5b). These data indicate that oscillatory activities from individual brain areas could adequately represent the three behavior categories.

We estimated the predictor importance for different frequency bands from all the brain areas. Consistent with the better performance using the power predictors, the predictor importance for power was consistently higher than that for coherence (Fig. S7c online). In the classification of wall and center, the two most important power features with the highest values were dHPC gamma and PFC gamma (Fig. 5c). In the classification of in and out of the garden, the two most important features were dHPC theta and dHPC gamma (Fig. 5c). In the classification of explored and unexplored areas (Fig. 5c), the two most important features were PFC delta and dHPC theta. We then performed classification separately in the VEH and DZP groups. In both groups, these 24 features could perform classifications accurately (Fig. 5d). Predictors with the highest prediction importance were also from the dHPC and PFC (Fig. S7d online). These data reveal that individual oscillatory activities in the dHPC and the PFC could predict different exploratory patterns, and they had better representations than the cross-area synchronized oscillations.

3.7. Initiation of exploration is modulated by dHPC and PFC power

The onset of exploration behavior in the arena is determined by the internal exploratory volition and drive. During the 80 min experiment, some animals stayed in the home for the entire duration with minimal exploratory activity, i.e., around the opening only. This exploration variability reflects the behavioral traits and different modes of processing on initializing exploration. To understand the neural activities that modulate the internal exploratory motivation prior to the emergence of exploration, we examined the theta activities during the baseline period before the shutter opening in the mice that exhibited exploration behavior (explorer group) and in those that only stayed in the home and never entered the arena during the entire test time (home-only group). During the initial 15 min after the shutter opening, the explorer animals mostly spent time in the home with minimal excursion in the arena.

In the PFC, we observed different theta activity patterns after the shutter opening between the explorer mice and the home-only mice (group-by-time interaction: $F_{(5,\ 50)} = 4.07$, $P = 0.0036$; Fig. 6a). The theta power decreased after the shutter opening in the explorer mice, and the power remained unchanged in the home-only mice. In the DZP treatment group, the explorer and home-only mice decreased in theta power (Fig. 6b), although no effect of group-by-time interaction was found. These results indicate that initiation of exploration is associated with decreased theta power in the PFC. In the dHPC, the theta power changes over time in the explorer mice were different from those in the home-only mice (group-by-time interaction: $F_{(5,\ 50)} = 5.868$, $P = 0.0002$; Fig. 6c) after the shutter opening. The explorer mice showed an increase in theta power, and the home-only mice did not show changes in theta power. In the DZP group, the same pattern was found (group-by-time interaction: $F_{(5,\ 30)} = 6.78$, $P = 0.0002$; Fig. 6d). These data show that initiation of the exploration is associated with increased theta power in the dHPC. Therefore, an exploration into unknown territory is modulated by the coordination of PFC and HPC oscillations with the two areas working synergistically to determine the emergence of the exploration and the individual variabilities.

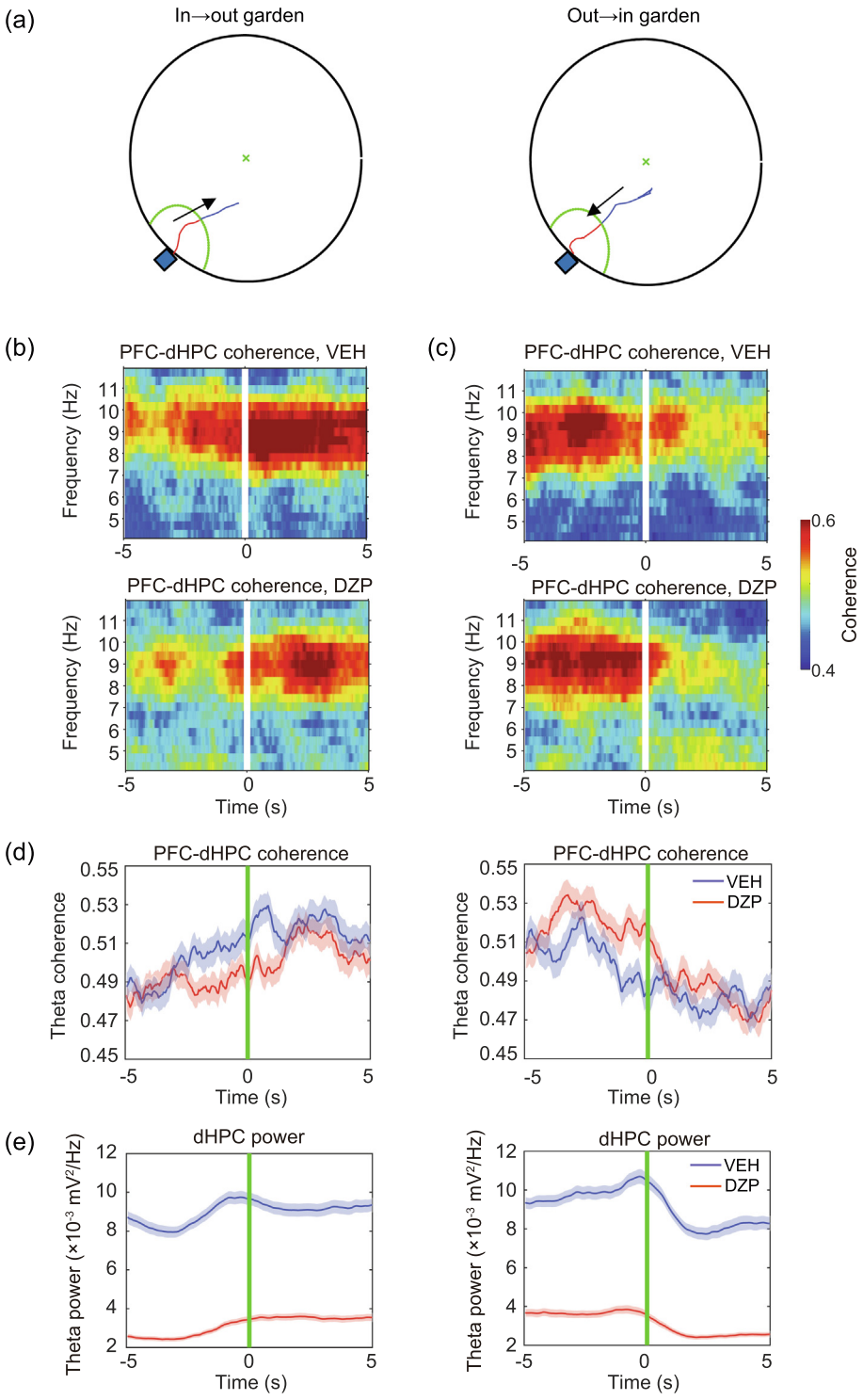

Fig. 4. PFC–dHPC synchronization signals the in/out garden transition. (a) Example showing that the mice transit from the garden area into the arena (in → out the garden) and from the outside-garden area into the garden (out → in the garden). The garden area is marked by a curved line around the home. Blue box represents home connected to the arena through small opening on the arena wall. Green × represents the arena center. (b, c) Time-dependent coherence between dHPC and PFC during the transition of in/out garden. Top row, VEH group. Bottom row, time DZP group. (b) in → out transition. (c) out → in transition. (d) Averaged theta band (4–12 Hz) coherence before and after garden transition. Left, in → out transition, paired *t*-test, DZP, $t_{(143)} = 2.8$, $P = 0.0058$; VEH $t_{(125)} = 3.46$, $P < 0.0001$. Right, out → in transition: paired *t*-test, DZP $t_{(139)} = 5.86$, $P < 0.0001$; VEH $t_{(128)} = 3.23$, $P = 0.0016$. (e) dHPC theta power during in/out garden transitions. In → out: paired *t*-test, DZP $t_{(143)} = 9.9$, $P < 0.00001$; VEH $t_{(125)} = 2.9$, $P = 0.0045$. Out → in: paired *t*-test, DZP $t_{(139)} = 10.05$, $P < 0.00001$; VEH $t_{(128)} = 7.24$, $P < 0.00001$. The data of shaded areas are shown as mean ± standard error of the mean (SEM).

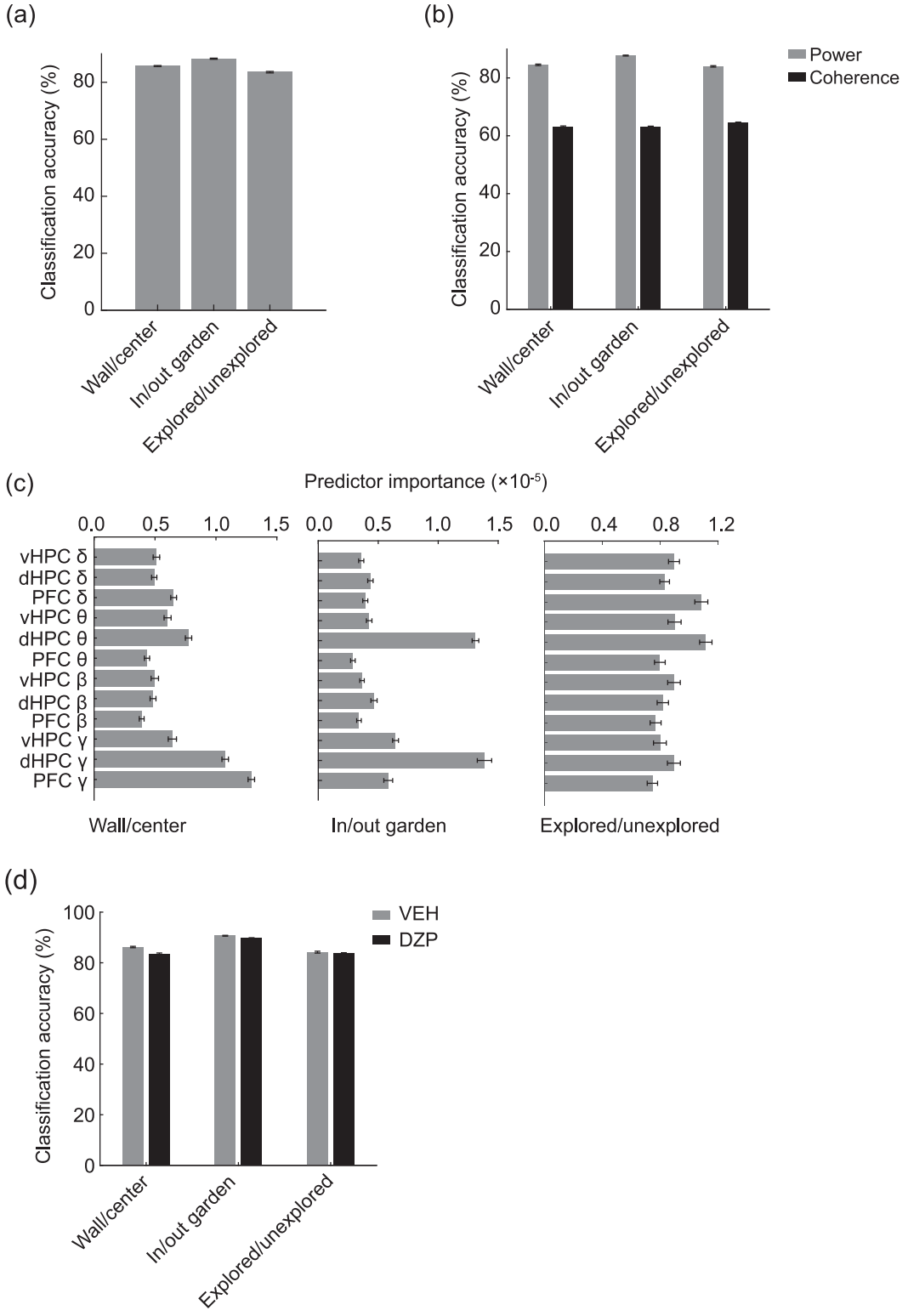

Fig. 5. Classification of multiple exploration categories using individual dHPC and PFC oscillatory activities. (a) Successful classification of wall vs. center, in vs. out of the garden, and explored vs. unexplored areas using 24 oscillatory features extracted from four frequency bands out of the three brain areas. (b) Classification performance using individual (power, 12 features) and synchronized (coherence, 12 features) oscillations. (c) Predictor importance estimations for each oscillatory feature using the power under three exploration categories. (d) Classification of exploration categories in VEH and DZP group separately. The data are shown as mean ± standard deviation (SD).

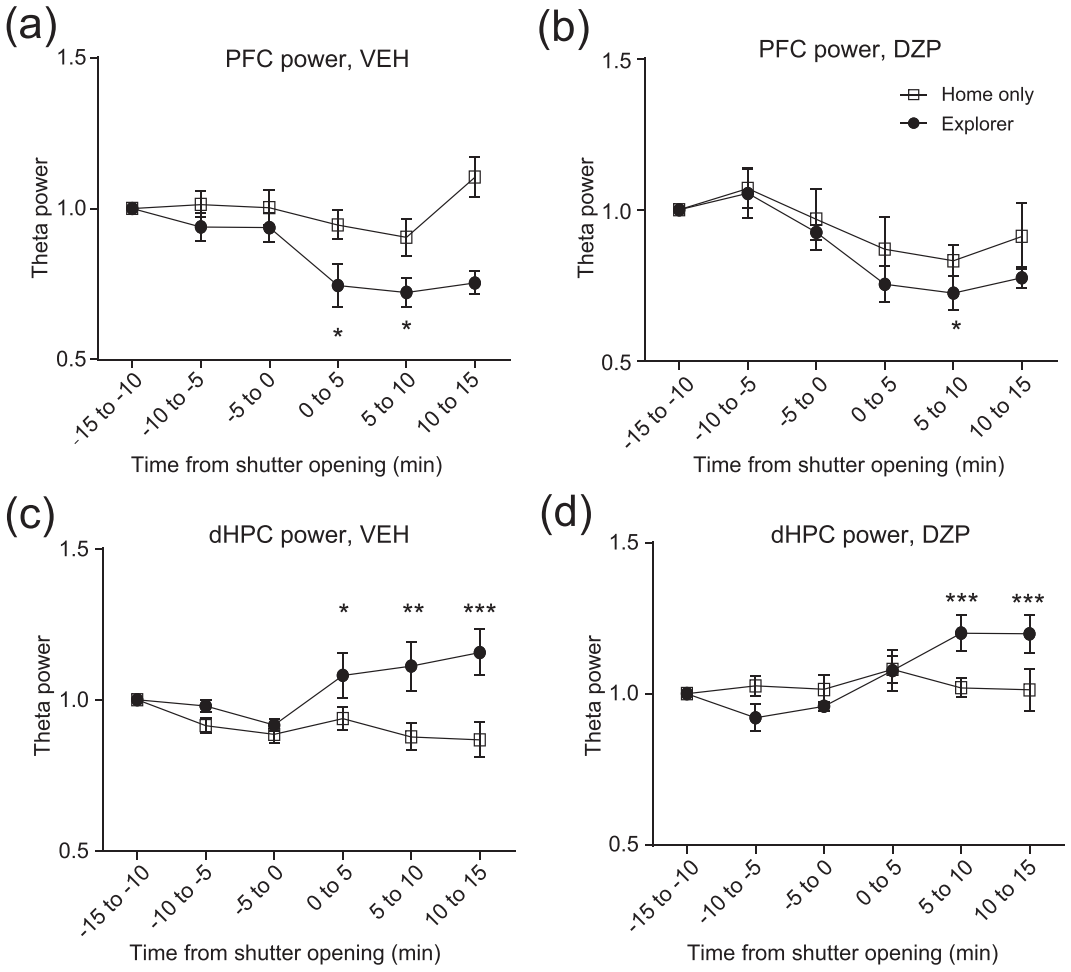

Fig. 6. Modulation of exploration initiation by coordinated PFC and dHPC theta oscillations. (a, b) Lowered PFC theta power in mice showing active exploration, whereas PFC power was not changed in mice that stayed in the home only after shutter opening. The power was normalized by the data in the first 5 min in the home. (a) VEH group; (b) DZP group. (c, d) Enhanced dHPC power in the mice showing active exploration, whereas dHPC power was not changed in the mice that stayed in the home only after shutter opening. (c) VEH group. (d) DZP group. * $P < 0.05$, ** $P < 0.01$, *** $P < 0.001$, −5 to 0 min compared with other times, Fisher's LSD. The data are shown as mean ± standard error of the mean (SEM).

4. Discussion

4.1. Dynamics of exploration

The naturalistic setup consisting of a large arena and a home base allowed observations of sequential excursions in an unknown territory, a similar pattern observed in other animals [26–29]. We provided computational methods to quantify the complexity and extent of the exploration in unknown environments. In order to characterize the extent of the exploratory dynamics, we defined the cumulative occupancy entropy to understand the accumulating exploratory pattern and the local occupancy entropy to quantify the exploration in a short time. Both entropy measurements revealed a trend of increased exploration over time, demonstrating that exploration shows a buildup pattern. The cumulative entropy showed increased occupancy of the arena when the exploration was perturbed by DZP during the early exploration stage. The local entropy showed a decreased occupancy with a concentrated distribution during the later exploration stage. Thus, the two entropy tools can disclose selective changes in the exploratory dynamics when the exploration behavior is under pharmacological perturbation.

We further defined the explored and unexplored areas during each excursion in the arena. The choice of explored path reflects that navigational preference is built upon prior experience that has been established during previous excursions. The choice of unexplored path reflects an incremental expansion of familiar areas into unknown areas. Our analyses showed that the proportion of unexplored areas decreased with time, indicating an increased familiarity. The local entropy in unexplored areas increased with time regardless of drug treatment, demonstrating a continued active exploratory capacity to cover more unknown areas.

4.2. dHPC and PFC oscillatory activities in exploration

Our findings reveal a prominent correlation between the dHPC theta activity and the occupancy entropy. dHPC theta activity has been found in spatial navigation [11,30–32] and contextual memory [33,34]. In traveling between the garden area, an area near the home, and the outside area, we found that dHPC–PFC synchronization signaled the transitions. The increased theta coherence demonstrated that spatial processing in the outside space was accompanied by increased synchrony between the PFC and dHPC. We performed machine learning classifications using LFP power and coherence features on a range of behavioral dimensions, including wall/center, in/out of the garden, and explored/unexplored territories. Results indicated that power predictors outper-

formed coherence predictors, demonstrating that LFP power itself possesses good representation properties. Unlike spike data, LFP signals reflect an ensemble of neuronal, dendritic, and synaptic activities in the local neuronal neighborhood, and slow waves of LFP may be influenced by volume conduction [35]. Nonetheless, we found that dHPC and PFC oscillatory features can sufficiently serve as important predictors in classifying various aspects of the exploratory behavior.

4.3. Individuality on free exploration

The emergence of active exploration in the unknown territory vs. reluctance to enter the arena and the preference of homestay reflect the individuality in exploration. In a large enriched environment, genetically identical inbred mice show diverged exploratory patterns of location landmarks over time, marking the emergence of individuality in exploration [36]. Exploratory activity correlates with adult hippocampal neurogenesis [37], a developmental process responsible for shaping the neural circuit. Our findings of comodulation of exploratory initialization by the PFC and dHPC suggest that individualized preference is a reflection of neural plasticity and may be controlled at the level of the neural circuit.

dHPC–PFC synchronization facilitates neuronal communications [38] and consolidates experience-dependent processes [32]. The willingness to explore in an unforeseen territory may be driven by curiosity, which is determined by several motivational intents, including novelty seeking, learning, and uncertainty resolving. Co-occurrence of decreased PFC and increased dHPC theta activities suggests that multiple modalities influence the emergence of exploration. These hypotheses need to be tested further to understand how different motivational modalities influence free exploration and the coordination of brain areas involved in the exploratory behavior.

Conflict of interest

The authors declare that they have no conflict of interest.

Acknowledgments

This work was supported by the National Natural Science Foundation of China (32070985), Shenzhen-Hong Kong Institute of Brain Science-Shenzhen Fundamental Research Institutions (NYKFKT20190018), and Shenzhen Key Laboratory of Translational Research for Brain Diseases (ZDSYS20200828154800001).

Author contributions

Cornelius Gross, Bailu Si, and Yang Zhan conceived and supervised the project. Yang Zhan performed the experiment. Wenxiu Dong, Hongbiao Chen, Timothy Sit, Yechao Han, Fei Song, Bailu Si, and Yang Zhan analyzed the data. Alexei Vyssotski supplied the recording hardware. Yang Zhan wrote the manuscript.

Appendix A. Supplementary materials

Supplementary materials to this article can be found online at https://doi.org/10.1016/j.scib.2021.05.018.

References

[1] Berlyne DE. Novelty and curiosity as determinants of exploratory behaviour. B J Psychol-Gen Sect 1950;41:68–80.
[2] Loewenstein G. The psychology of curiosity: a review and reinterpretation. Psychol Bull 1994;116:75–98.
[3] Little D, Sommer F. Learning and exploration in action-perception loops. Front Neural Circuits 2013;7:37.
[4] Fonio E, Benjamini Y, Golani I. Freedom of movement and the stability of its unfolding in free exploration of mice. Proc Natl Acad Sci USA 2009;106:21335–40.
[5] Koolhaas JM, Korte SM, De Boer SF, et al. Coping styles in animals: current status in behavior and stress-physiology. Neurosci Biobehav Rev 1999;23:925–35.
[6] Roberts WW, Dember WN, Brodwick M. Alternation and exploration in rats with hippocampal lesions. J Comp Physiol Psychol 1962;55:695–700.
[7] Adhikari A, Topiwala MA, Gordon JA. Synchronized activity between the ventral hippocampus and the medial prefrontal cortex during anxiety. Neuron 2010;65:257–69.
[8] Adhikari A, Topiwala MA, Gordon JA. Single units in the medial prefrontal cortex with anxiety-related firing patterns are preferentially influenced by ventral hippocampal activity. Neuron 2011;71:898–910.
[9] Lee AT, Cunniff MM, See JZ, et al. Vip interneurons contribute to avoidance behavior by regulating information flow across hippocampal-prefrontal networks. Neuron 2019;102:1223–34.
[10] Benchenane K, Peyrache A, Khamassi M, et al. Coherent theta oscillations and reorganization of spike timing in the hippocampal-prefrontal network upon learning. Neuron 2010;66:921–36.
[11] Jones MW, Wilson MA. Theta rhythms coordinate hippocampal–prefrontal interactions in a spatial memory task. PLoS Biol 2005;3:e402.
[12] Leussis MP, Bolivar VJ. Habituation in rodents: a review of behavior, neurobiology, and genetics. Neurosci Biobehav Rev 2006;30:1045–64.
[13] Gordon G, Fonio E, Ahissar E. Emergent exploration via novelty management. J Neurosci 2014;34:12646–61.
[14] Zhan Y. Theta frequency prefrontal–hippocampal driving relationship during free exploration in mice. Neuroscience 2015;300:554–65.
[15] Jain A, Dvorkin A, Fonio E, et al. Validation of the dimensionality emergence assay for the measurement of innate anxiety in laboratory mice. Eur Neuropsychopharmacol 2012;22:153–63.
[16] Drai D, Golani I. See: a tool for the visualization and analysis of rodent exploratory behavior. Neurosci Biobehav Rev 2001;25:409–26.
[17] Lipkind D, Sakov A, Kafkafi N, et al. New replicable anxiety-related measures of wall vs. center behavior of mice in the open field. J Appl Physiol 2004;97:347–59.
[18] Mitra P, Bokil H. Observed brain dynamics. Oxford: Oxford University Press; 2007.
[19] Loh W-Y. Regression trees with unbiased variable selection and interaction detection. Stat Sin 2002;12:361–86.
[20] Breiman L, Friedman J, Stone CJ, et al. Classification and regression trees. Florida: CRC Press; 1984.
[21] Benjamini Y, Fonio E, Galili T, et al. Quantifying the buildup in extent and complexity of free exploration in mice. Proc Natl Acad Sci USA 2011;108:15580–7.
[22] Tchernichovski O, Benjamini Y, Golani I. The dynamics of long-term exploration in the rat. Biol Cybern 1998;78:423–32.
[23] Moser EI, Moser M-B, McNaughton BL. Spatial representation in the hippocampal formation: a history. Nat Neurosci 2017;20:1448–64.
[24] Schomaker J. Unexplored territory: beneficial effects of novelty on memory. Neurobiol Learn Mem 2019;161:46–50.
[25] Zhan Y, Paolicelli RC, Sforazzini F, et al. Deficient neuron-microglia signaling results in impaired functional brain connectivity and social behavior. Nat Neurosci 2014;17:400–6.
[26] Burke CJ, Whishaw IQ. Sniff, look and loop excursions as the unit of "exploration" in the horse (*Equus ferus caballis*) when free or under saddle in an equestrian arena. Behav Processes 2020;173:104065.
[27] Stewart A, Cachat J, Wong K, et al. Homebase behavior of zebrafish in novelty-based paradigms. Behav Process 2010;85:198–203.
[28] Hills TT, Todd PM, Lazer D, et al. Exploration versus exploitation in space, mind, and society. Trends Cogn Sci 2015;19:46–54.
[29] Vyssotski AL, Dell'Omo G, Dell'Ariccia G, et al. EEG responses to visual landmarks in flying pigeons. Curr Biol 2009;19:1159–66.
[30] Leutgeb JK, Leutgeb S, Treves A, et al. Progressive transformation of hippocampal neuronal representations in morphed environments. Neuron 2005;48:345–58.
[31] Kleinfeld D, Deschênes M, Ulanovsky N. Whisking, sniffing, and the hippocampal θ-rhythm: a tale of two oscillators. PLoS Biol 2016;14:e1002385.
[32] Lever C, Burton S, Jeewajee A, et al. Environmental novelty elicits a later theta phase of firing in CA1 but not subiculum. Hippocampus 2010;20:229–34.

[33] Fanselow MS. Contextual fear, gestalt memories, and the hippocampus. Behav Brain Res 2000;110:73–81.
[34] Wirt RA, Hyman JM. ACC theta improves hippocampal contextual processing during remote recall. Cell Rep 2019;27:2313–27.
[35] Sirota A, Montgomery S, Fujisawa S, et al. Entrainment of neocortical neurons and gamma oscillations by the hippocampal theta rhythm. Neuron 2008;60:683–97.
[36] Freund J, Brandmaier AM, Lewejohann L, et al. Emergence of individuality in genetically identical mice. Science 2013;340:7566–9.
[37] Clemenson GD, Deng W, Gage FH. Environmental enrichment and neurogenesis: from mice to humans. Curr Opin Behav Sci 2015;4:56–62.
[38] Colgin LL. Mechanisms and functions of theta rhythms. Annu Rev Neurosci 2013;36:295–312.

Wenxiu Dong is a post-doctoral reseacher at the Brain Cognition and Brain Disease Institute, Shenzhen Institutes of Advanced Technology, Chinese Academy of Sciences. He received his Ph.D. degree in Physics from the University of Science and Technology of China. His research interest focuses on decision-making during a virtual navigation task.

Bailu Si is a professor at the School of Systems Science of Beijing Normal University. He received a Ph.D. degree in Theoretical Neurophysics from Bremen University, Germany. His research interest includes computational neuroscience and brain-inspired intelligence.

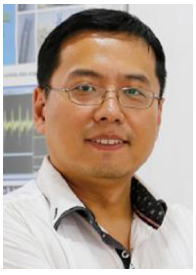

Yang Zhan is a professor at the Brain Cognition and Brain Disease Institute, Shenzhen Institutes of Advanced Technology, Chinese Academy of Sciences. He received his Ph.D. degree from University of Cambridge, UK. His main research interest focuses on systems neuroscience and neural engineering.